[Article] www.whxb.pku.edu.cn

简易方法制备交叉碳纳米管-石墨烯异质结

甘 霖 刘 松 李丹娜 谷 航 曹 阳
申 茜 王振兴 王 青 郭雪峰*
(北京大学化学与分子工程学院, 分子动态与稳态结构国家重点实验室, 北京分子科学国家实验室, 北京 100871)

摘要: 该研究发展了一种通过两次高分子辅助转移和选择性氧等离子体刻蚀技术大量制备交叉碳纳米管-石墨烯异质结的无损方法. 拉曼光谱和导电性测试证明, 制备的单层石墨烯薄片在大面积范围内质量均一、导电性好. 而且, 该论文所讨论的单层石墨烯的生长和随后的器件制备也提供了大面积制备石墨烯薄片图案化的可重复性方法. 该方法与传统的薄膜技术兼容, 只需简易的几步便可把图案化的石墨烯集成到大规模的微电子器件回路中, 有希望实现流线型和自动化的石墨烯微电子器件的大量生产. 这些研究结果为进一步制备分子整流器和其它功能纳米/分子电子器件提供了技术基础.

关键词: 石墨烯; 纳米/分子电子器件; 单壁碳纳米管; 分子整流器; 纳米转移印刷
中图分类号: O646

Facile Fabrication of Crossed Nanotube-Graphene Junctions

GAN Lin LIU Song LI Dan-Na GU Hang CAO Yang
SHEN Qian WANG Zhen-Xing WANG Qing GUO Xue-Feng*
(*Beijing National Laboratory for Molecular Sciences, State Key Laboratory for Structural Chemistry of Unstable and Stable Species, College of Chemistry and Molecular Engineering, Peking University, Beijing 100871, P. R. China*)

Abstract: In this study, a nondestructive method to mass produce crossed nanotube-graphene junctions through twice polymer-mediated transfer techniques and selective oxygen plasma etching was developed. Raman and conductance measurements demonstrated that the quality and electrical properties of the single-layer graphene (SLG) sheets are uniform over a large area. Furthermore, SLG synthesis and device fabrication discussed here also provide a reproducible method to pattern graphene sheet arrays for making graphene-based microdevices over large areas and with high yield, which is compatible with standard thin film technologies and allows SLG to be integrated into large scale electronics circuitry within several simple steps that can be easily streamlined and automated. These results might offer grounds for the creation of a wide variety of molecular rectifiers and other functional nano/molecular devices.

Key Words: Graphene; Nano/molecular devices; Single-walled carbon Nanotube; Molecular rectifier; Nanotransfer printing

The engineering of molecular electronic devices relies on the control and exploration of the electronic properties of the junctions. These properties include the intrinsic electronic device functions as well as the ability of the molecules to interact with the electrodes. Among these functions, rectification behavior is one of the most exciting device functions, which was first envisioned by Aviram and Ratner[1]. The Aviram-Ratner molecular diode consists of a donor and an acceptor separated with a σ

Received: November 24, 2009; Revised: January 14, 2010; Published on Web: February 24, 2010.
*Corresponding author. Email: guoxf@pku.edu.cn; Tel: +86-10-62757789.
The project was supported by the FANEDD (2007B21, B08001, 2009A01), National Key Basic Research Program of China (973) (2009CB623703), and National Natural Science Foundation of China (50873004, 50821061, 20833001).
全国高等学校优博论文作者专项基金(2007B21)、高等学校学科创新引智计划(B08001)、北京市科技新星(2009A01)、国家重点基础研究发展计划(973)(2009CB623703)和国家自然科学基金(50873004, 50821061, 20833001)资助项目

bridge in which the forward current is from the acceptor to the donor. To date, most experimental studies of molecular diodes have been carried out using Langmuir-Blodgett films[2–3] and self-assembled monolayers (SAMs)[4–6]. However, the study of the diode behaviors in these molecular junctions is significantly limited due to the requirement of sophisticated and time-consuming device fabrication and the unavailability of the molecules with desired structures.

Another efficient approach to realize the rectification behaviors at the molecular level is to form T- or Y-shaped heterojunctions between different nanomaterials. In the past decade, much effort has been made to create nano-heterojunctions between nanotubes (NTs) and nanowires (NWs) because they could provide building blocks for nanoelectronics and nanophotonics[7–9]. Although several types of nano-heterojunctions between nanotubes and nanowires have been made[8–13], the key question of the fabrication of the nano-heterojunctions remained a significant challenge. This is due to the difficulty of direct growth of T- or Y-shaped heterojunctions. In this work, we report a facile technique for producing a large number of crossed nanotube-graphene heterojunctions through a nondestructive polymethyl methacrylate (PMMA)-mediated nanotransfer printing appr oach[14–15] and selective oxygen plasma etching. Then through only one-step electron beam lithography, we can easily fabricate the corresponding nanodevices.

Single-walled carbon nanotubes (SWNTs)[16] and single-layer graphene (SLG)[17], two star molecules of carbon nanomaterials, have been proposed as the ideal systems for nanoelectronics and molecular electronics in both academic and industrial communities[18–22]. Nanojunctions consisting of two crossed SWNTs were fabricated to form two- and three-terminal devices, which showed a rectifying Schottky barrier[23]. However, a question remains: what will happen when individual SWNTs are joined with SLG to form multi-terminal devices and, ultimately, complex circuits? To answer this question, in this study we focus on the technical development of building SWNT-SLG heterojunctions formed by graphene that lie across nanotubes on silicon wafer substrates (Fig.1).

1 Results and discussion

A schematic procedure for fabricating the SWNT-SLG heterojunctions is given in Fig.2. Although the final SWNT-SLG heterojunctions are obtained through 9 steps, each step is quite simple without either traditional photolithography or complicated electron beam lithography. Within one or two days, one could use this facile procedure to mass produce SWNT-SLG heterojunctions. Firstly we synthesize SLG through a chemical vapor deposition process (CVD). Currently, several promising synthesis methods have been developed to grow SLG. These include epitaxial graphene on SiC[24–25], graphene oxide reduction[26–27], direct growth out of thin nickel film[28–29], and most recently on copper foils[30]. Among these methods, the latest copper foil-based synthesis is the most effective in producing large continuous SLGs with promising electrical properties. In our procedure, we use 25 μm thick copper films (Alfa Aesar) to grow our SLG. The basic mechanism is similar to that recently reported in Ref. [30]. Before graphene growth, Cu films were immersed in acetic acid at 40 ℃ for 15 min in order to remove most of the copper oxide. We found that this is an important pretreatment because removal of the copper oxide prior to growth improves the quality of the copper film and thus the quality of SLG. A typical growth process is listed below. A quartz substrate with the Cu film was loaded into the furnace. Then the system was evacuated and heated to 1000 ℃ under a 10 $cm^3 \cdot min^{-1}$ flow of H_2 at a pressure of about 50 Pa. After stabilizing the Cu film at the desired temperature, we introduced 1.1 $cm_3 \cdot min^{-1}$ of CH_4 for 5–10 min at a pressure of about 60 Pa. After the growth the substrates

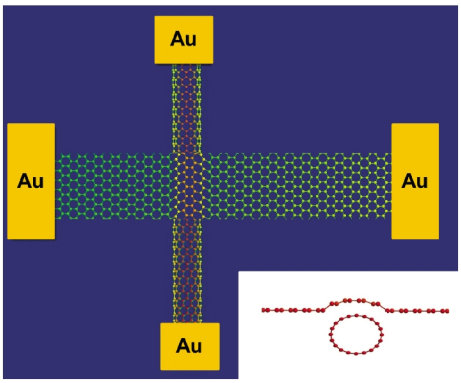

Fig.1 Schematic structure of crossed SWNT-SLG heterojunctions

Inset shows the assumption that deformations in both SWNT and SLG could happen at the junction due to their interaction with SiO_2 substrates.

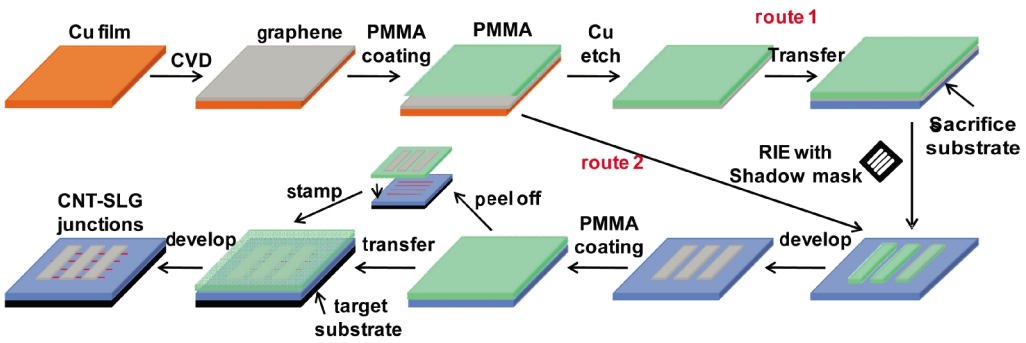

Fig.2 Schematic representation of the fabrication procedure to form crossed nanotube-graphene heterojunctions

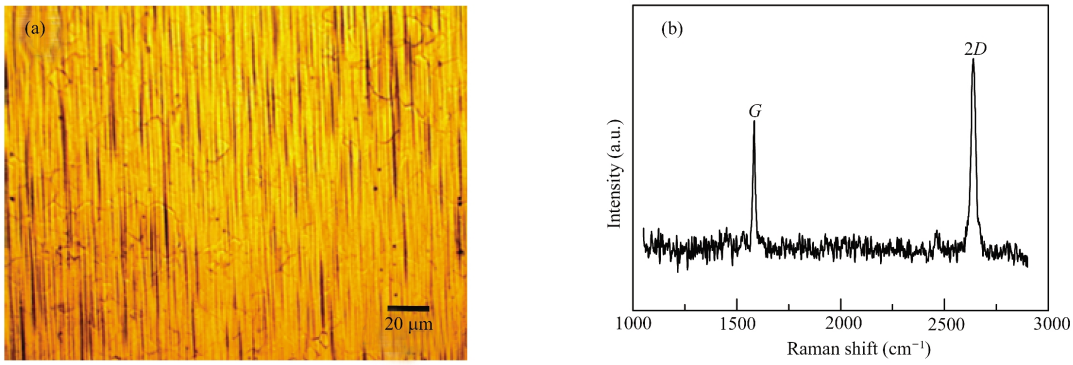

Fig.3 (a) A contrast-enhanced optical image of a typical sample substrate after graphene growth, (b) a representative Raman spectrum of the grown graphene

were then cooled down to room temperature for the next transfer step. Fig.3(a) shows a contrast-enhanced optical image of a typical sample substrate after graphene growth. We found that graphene was continuous across the visible Cu grains as demonstrated below. Fig.3(b) presents a Raman spectrum that is representative of the grown graphene. A single symmetric 2*D* peak (full width at half-maximum ca 34 cm^{-1}), a small *G*/2*D* ratio, and a negligible *D* peak are observed, which strongly suggest that our graphene is a single layer and the quality of the sheet is not significantly affected by the visible features of the Cu film[30].

After graphene growth, polymer PMMA with 300 nm thickness was spin coated on the Cu films. The whole samples were then immersed into a continually refreshed saturated solution of iron nitrate for an enough long time to remove the Cu substrates. The resultant transparent sheet floating in the aqueous solution was transferred to a sacrifice silicon substrate. To demonstrate the efficiency of the PMMA-mediated transfer technique, we simply tested the quality of graphene after removing PMMA in a boiling acetone solution. As shown in Fig.4(a), this method allows us to transfer large-area continuous high-quality graphenes with only small residues to any kinds of substrates as confirmed by Raman measurements (see below). To form graphene sheets, we directly applied an oxygen plasma etching process (oxygen: 19 $cm^3 \cdot min^{-1}$, pressure: 35 Pa, power: 50 W) for 2.5 min without

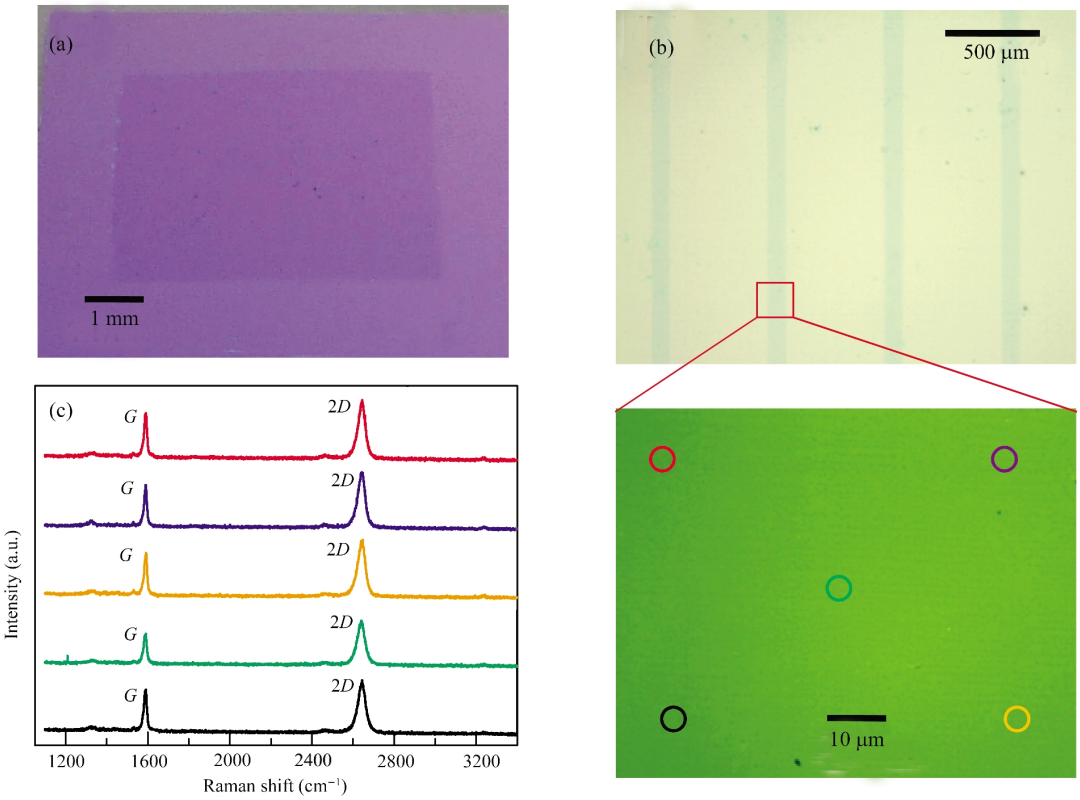

Fig.4 (a) An optical image of large-area graphenes after PMMA-mediated nanotransfer process, (b) an optical image of graphene sheet array after oxygen plasma etching and the zoomed-in image of the part labeled by a red square, (c) Raman spectra obtained from the marked spots with the corresponding colored circles

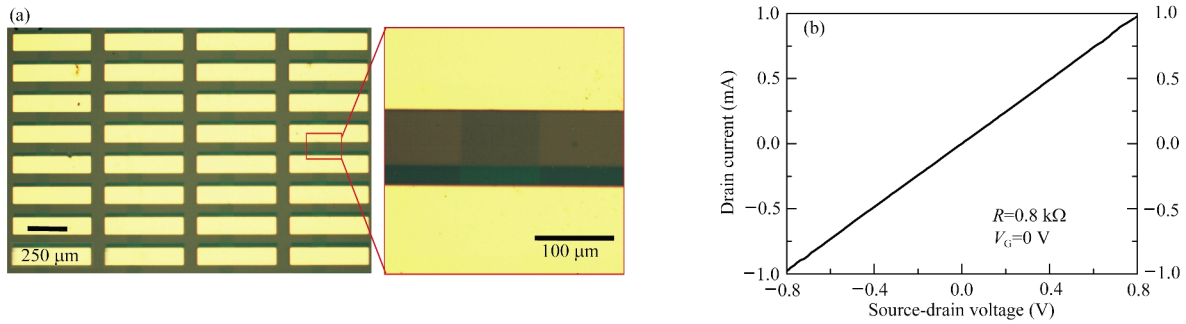

Fig.5 (a) Schematic representation of the SLG device array and the enlarged optical image of a representative device, (b) a representative electronic property of the same device

removing PMMA thin films after the transfer step to etch away the unprotected graphene beneath the exposed PMMA through a shadow mask. Then after removing the remaining PMMA in a boiling acetone solution, graphene sheets with desired patterns were obtained. Fig.4(b) shows an optical image of the resulting sheet array with ca 100 μm width separated by ca 500 μm. In principle, graphene microarrays with any kinds of patterns could be easily obtained through this flexible process, depending on the design of the shadow mask. A zoomed-in optical image of one part is also shown in Fig.4(b). This contrast-enhanced image confirms that the surface of SLG sheets is very clean without obvious damages and any visible residues on top of them. To further evaluate the quality and uniformity of the transferred graphenes, we used Raman spectroscopy to characterize them. Fig.4(c) shows the corresponding Raman spectra from the marked circles with different colors in Fig.4(b). Surprisingly, the resulting graphene sheets show the uniform Raman signature over large areas and remain the same original quality as shown in Fig. 3(b). Based on the Raman analysis, we estimated the SLG coverage to be a minimum of 93%[30]. The Raman measurements as well as the optical characterization demonstrate that this nanotransfer and oxygen plasma etching process is useful for making large-area high-quality graphene microdevices in a nondestructive manner. We found that the sequential transfer and oxygen plasma etching process is important. If the oxygen plasma etching is straightly applied on the Cu films without the transfer step as shown in Fig.2 (Route 2), extensive damages of the graphene sheets can occur probably due to the fragility of Cu films.

To transfer graphene sheets to the desired substrates, we performed another PMMA-mediated transfer step. Similarly, 300 nm PMMA was spin coated on the sacrifice silicon substrates. After immersing the whole sample in the aqueous solution of potassium hydroxide (1.0 mol·L^{-1}) at the temperature of 80 ℃ for half an hour[15], PMMA thin films together with the graphene sheet array can be peeled off from the sacrifice substrates. Then the floating transparent PMMA thin films were transferred onto the target silicon substrates with 300 nm thermally grown silicon oxide. After dissolving PMMA in a boiling acetone, the graphene sheets were released to the target substrate. To test the electronic properties of these graphene sheets, we made the transistor arrays through a simple thermal evaporation. One key advantage of our device fabrication process is its high yield and uniform electronic properties. In order to show this, we fabricated 200 devices on a single substrate over a large area (about 8 mm×6 mm). A representative device schematic is shown in Fig. 5 (a). Only 3 out of 200 devices are obviously damaged and all other devices are conductive, showing the yield as high as 98%. Fig.5(b) shows the corresponding electronic property of one representative device shown in Fig.5(a). Based on the data, we estimate the average sheet resistance to be about 0.7−1.2 kΩ. The high yield of the highly conductive devices demonstrated here and the uniform Raman features shown in Fig.4(c) confirm the continuous growth of SLG over a large area and the efficiency of our nondestructive transfer technique.

After proving the high conductivity of the resulting graphene sheets, we finally transferred them to the silicon wafer substrates with pre-grown well-aligned ultralong SWNT arrays. Well-aligned ultralong SWNTs were grown through a standard CVD process on silicon wafers with a 300 nm SiO_2 layer[31−32] and with different marks, which help find SWNTs under SEM. With care, graphene sheets with desired patterns can be precisely positioned perpendicular to SWNT arrays, thus forming high-density crossed SWNT-SLG junctions. Fig.6(a) shows such a SEM image of crossed SWNT-SLG junctions with distinctive marks, showing the average density of ca 3 junctions per 100 μm. With the aid of these marks, the corresponding nanodevices based on these SWNT-SLG junctions were then fabricated through only one-step electron beam lithographic process. Fig.6(b) shows the SEM images of a representative nanodevice, clearly showing that SLG lies across SWNT. It is well-known that SWNTs may be metallic or semiconducting, depending on their chirality[33−34]. At room temperature, metallic SWNTs have a finite conductance that is nearly independent of V_G. Semiconducting SWNTs are found to be *p*-type, conducting at negative V_G and insulating at positive V_G. However, graphene at the micrometer scale shows only semimetallic properties due to its zero bandgap[18−22]. Therefore, our crossed SWNT-SLG junctions can be composed of one metallic SWNT and one SLG (MM), or one semiconducting SWNT and one SLG (MS). We expect that a rectifying Schottky barrier could be formed when the semiconducting SWNT is con-

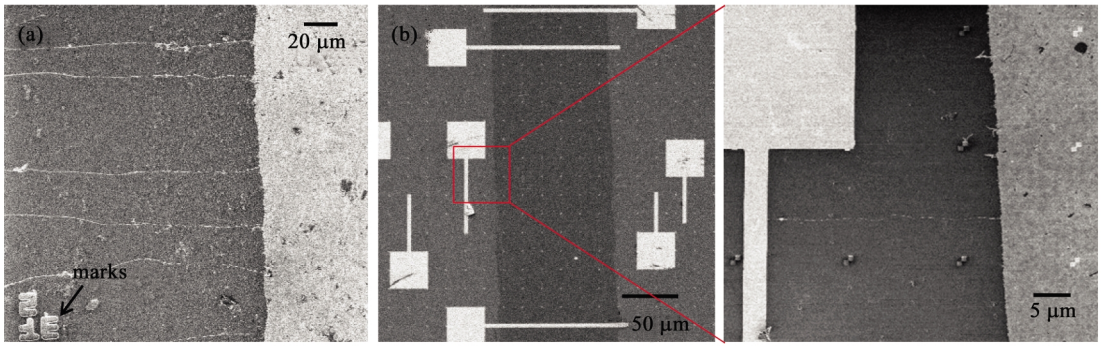

Fig.6 (a) A SEM image of crossed SWNT-SLG junctions, (b) SEM images of a representative nanodevice

nected with the semimetallic graphene. This potential initiates our great attention to exploring the foreseen and unforeseen properties on these SWNT-SLG junctions. The electrical characterization is still in progress.

2 Conclusions

In this study, we detailed a nondestructive method to mass produce crossed SWNT-SLG junctions through twice PMMA-mediated transfer techniques and selective oxygen plasma etching. SLGs used here were grown over large areas on Cu films by a CVD method. Then graphene sheet array with desired patterns were made by applying oxygen plasma etching through a shadow mask after the first transfer step. Raman and conductance measurements show that the quality and electrical properties of our SLG sheets are uniform over a large area. Finally, crossed SWNT-SLG junctions can be easily achieved by transferring the graphene sheet array onto the target substrates with well-aligned SWNT arrays. Characterization of the electrical properties of nanodevices based these heterojunctions is underway and will be reported in due time. In addition to forming crossed SWNT-SLG junctions, SLG synthesis and device fabrication discussed in this article also provides a reliable method to pattern graphene sheet arrays for making graphene-based microdevices over large areas and with high yield. This technique is compatible with standard thin film technologies and allows SLG to be integrated into large scale electronics circuitry within several simple steps that can be easily streamlined and automated. These results might offer the platform for the creation of a wide variety of molecular rectifiers and other functional nano/molecular devices.

References

1 Aviram, A.; Ratner, M. A. *Chem. Phys. Lett.*, **1974, 29**: 277
2 Martin, A. S.; Sambles, J. R.; Ashwell, G. J. *Phys. Rev. Lett.*, **1993, 70**: 218
3 Zhou, S. Q.; Liu, Y. Q.; Qiu, W. F.; Xu, Y.; Huang, X. B.; Li, Y. S.; Jiang, L.; Zhu, D. B. *Adv. Funct. Mater.*, **2002, 12**: 65
4 Chabinyc, M. L.; Chen, X. X.; Holmlin, R. E.; Jacobs, H.; Skulason, H.; Frisbie, C. D.; Mujica, V.; Ratner, M. A.; Rampi, M. A.; Whitesides, G. M. *J. Am. Chem. Soc.*, **2002, 124**: 11730
5 Elbing, M.; Ochs, R.; Koentopp, M.; Fischer, M.; von Hanisch, C.; Weigend, F.; Evers, F.; Weber, H. B.; Mayor, M. *Proc. Natl. Acad. Sci. U. S. A.*, **2005, 102**: 8815
6 Metzger, R. M. *Chem. Rev.*, **2003, 103**: 3803
7 Hochbaum, A. I.; Yang, P. *Chem. Rev.*, **2009**, DOI: 10.1021/cr900075v
8 Hu, J. T.; Ouyang, M.; Yang, P. D.; Lieber, C. M. *Nature*, **1999, 399**: 48
9 Zhang, Y.; Ichihashi, T.; Landree, E.; Nihey, F.; Iijima, S. *Science*, **1999, 285**: 1719
10 Meng, G. W.; Han, F. M.; Zhao, X. L.; Chen, B. S.; Yang, D. C.; Liu, J. X.; Xu, Q. L.; Kong, M. G.; Zhu, X. G.; Jung, Y. J.; Yang, Y. J.; Chu, Z. Q.; Ye, M.; Kar, S.; Vajtai, R.; Ajayan, P. M. *Angew. Chem. Int. Edit.*, **2009, 48**: 7166
11 Asaka, K.; Nakahara, H.; Saito, Y. *Appl. Phys. Lett.*, **2008, 92**: 023114
12 Luo, J.; Zhang, L.; Zhang, Y. J.; Zhu, J. *Adv. Mater.*, **2002, 14**: 1413
13 Rodriguez-Manzo, J. A.; Banhart, F.; Terrones, M.; Terrones, H.; Grobert, N.; Ajayan, P. M.; Sumpter, B. G.; Meunier, V.; Wang, M.; Bando, Y.; Golberg, D. *Proc. Natl. Acad. Sci. U. S. A.*, **2009, 106**: 4591
14 Xiao, S. X.; Tang, J. Y.; Beetz, T.; Guo, X. F.; Tremblay, N.; Siegrist, T.; Zhu, Y. M.; Steigerwald, M.; Nuckolls, C. *J. Am. Chem. Soc.*, **2006, 128**: 10700
15 Jiao, L. Y.; Fan, B.; Xian, X. J.; Wu, Z. Y.; Zhang, J.; Liu, Z. F. *J. Am. Chem. Soc.*, **2008, 130**: 12612
16 Iijima, S. *Nature*, **1991, 354**: 56
17 Novoselov, K. S.; Geim, A. K.; Morozov, S. V.; Jiang, D.; Zhang, Y.; Dubonos, S. V.; Grigorieva, I. V.; Firsov, A. A. *Science*, **2004, 306**: 666
18 Feldman, A. K.; Steigerwald, M. L.; Guo, X.; Nuckolls, C. *Acc. Chem. Res.*, **2008, 41**: 1731
19 Dai, H. *Acc. Chem. Res.*, **2002, 35**: 1035
20 Guo, X.; Nuckolls, C. *J. Mater. Chem.*, **2009**, **19**: 5470
21 Geim, A. K.; Novoselov, K. S. *Nature Mater.*, **2007, 6**: 183
22 Zhang, Y.; Tan, Y. W.; Stormer, H. L.; Kim, P. *Nature*, **2005, 438**: 201
23 Fuhrer, M. S.; Nygard, J.; Shih, L.; Forero, M.; Yoon, Y. G.;

Mazzoni, M. S. C.; Choi, H. J.; Ihm, J.; Louie, S. G.; Zettl, A.; McEuen, P. L. *Science*, **2000, 288**: 494

24 Berger, C.; Song, Z. M.; Li, X. B.; Wu, X. S.; Brown, N.; Naud, C.; Mayou, D.; Li, T. B.; Hass, J.; Marchenkov, A. N.; Conrad, E. H.; First, P. N.; de Heer, W. A. *Science*, **2006, 312**: 1191

25 Dawlaty, J. M.; Shivaraman, S.; Chandrashekhar, M.; Rana, F.; Spencer, M. G. *Appl. Phys. Lett.*, **2008, 92**: 042116

26 Eda, G.; Fanchini, G.; Chhowalla, M. *Nat. Nanotech.*, **2008, 3**: 270

27 Dikin, D. A.; Stankovich, S.; Zimney, E. J.; Piner, R. D.; Dommett, G. H. B.; Evmenenko, G.; Nguyen, S. T.; Ruoff, R. S. *Nature*, **2007, 448**: 457

28 Reina, A.; Jia, X. T.; Ho, J.; Nezich, D.; Son, H. B.; Bulovic, V.; Dresselhaus, M. S.; Kong, J. *Nano Lett.*, **2009, 9**: 30

29 Kim, K. S.; Zhao, Y.; Jang, H.; Lee, S. Y.; Kim, J. M.; Kim, K. S.; Ahn, J. H.; Kim, P.; Choi, J. Y.; Hong, B. H. *Nature*, **2009, 457**: 706

30 Li, X. S.; Cai, W. W.; An, J. H.; Kim, S.; Nah, J.; Yang, D. X.; Piner, R.; Velamakanni, A.; Jung, I.; Tutuc, E.; Banerjee, S. K.; Colombo, L.; Ruoff, R. S. *Science*, **2009, 324**: 1312

31 Guo, X.; Xiao, S.; Myers, M.; Miao, Q.; Steigerwald, M. L.; Nuckolls, C. *Proc. Natl. Acad. Sci. U. S. A.*, **2009, 106**: 691

32 Liu, S.; Li, J. M.; Shen, Q.; Cao, Y.; Guo, X. F.; Zhang, G. M.; Teng, C. Q.; Zhang, J.; Liu, Z. F.; Steigerwald, M. L.; Xu, D. S.; Nuckolls, C. *Angew. Chem. Int. Edit.*, **2009, 48**: 4759

33 Dai, H. *Acc. Chem. Res.*, **2002, 35**: 1035

34 Liu, S.; Shen, Q.; Cao, Y.; Gan, L.; Wang, Z.; Steigerwald, M. L.; Guo, X. *Coord. Chem. Rev.*, **2009**, DOI: 10.1016/j.ccr.2009.11.007